

The Optical Modelling of Multi-Layer Structures for Thin-Film PV

Robert E Treharne* and Ken Durose

Stephenson Institute for Renewable Energy, University of Liverpool, Liverpool, UK. L69 7ZF.

*Corresponding Author R.Treharne@liverpool.ac.uk

Abstract

An open source transfer matrix method (TMM) implementation for calculating the optical response of thin-film multi-layer structures is developed and showcased in this work. It is applied to the optical optimisation of conventional CdTe thin-film solar cell configurations and used to highlight opportunities for experimental routes to improved device efficiency. The viability of ultra-thin Ag films as alternative contact materials for CdTe cells is also demonstrated.

1. Introduction

The Transfer Matrix Method (TMM) [1] for calculating the optical response (i.e. transmission, reflectance and absorbance) of a multi-layered stack of thin films is widely used in the design of dielectric mirrors and anti-reflection coatings. Implementation of the TMM is either achieved via proprietary software, which is commonly inflexible and expensive, or via inconsistent sets of scripts provided by independent researchers for use in highly specific scenarios. The objective of this work is to showcase the development of a powerful, flexible and open source implementation of the TMM, and demonstrate its use in the optimisation of multi-layer structures for thin-film photovoltaics. The following examples are documented:

1. Minimisation of reflectance from transparent conducting oxide single films.
2. Maximisation of short circuit current, J_{SC} , in thin-film CdTe solar cells.
3. Assessment of viability of ultra-thin silver transparent conductors as front electrodes for thin-film CdTe solar cells.

In each of the above examples the TMM implementation is successfully used to generate insight into how incremental gains into the optical performance of thin film photovoltaics can be achieved.

2. Experimental

The TMM was implemented using Python 2.7 and the relevant code scripts are fully accessible and downloadable from the online repository at <https://github.com/rtreharne/pytraml.git>.

The repository also includes user documentation and a series of examples to demonstrate the usage of the core TMM script "traml.py". The implementation incorporates the extensive open source optical database www.refractiveindex.info, which contains n and k data for over 400 materials [2].

A detailed review of how the transfer matrices are constructed and used to calculate transmittance and reflectance is presented in [3] pp. 176-181. The J_{SC} of modelled CdTe solar cell configurations is calculated using

$$J_{SC} = \int_{E_g}^{\infty} Q(E) \Phi(E) dE \quad (1)$$

where the external quantum efficiency, $Q(E)$, is defined by:

$$Q(E) = C(E) a(E) T_a \quad (2)$$

T_a being the transmittance at the interface between the solar cell's absorber layer and the preceding film stack. It is assumed throughout that the probability that a photon is absorbed within the absorber layer, $a(E)$, and the probability that it is converted into an electron, $C(E)$ are both equal to unity. The incident flux density, $\Phi(E)$, is consistent with that generated by an AM1.5 solar spectrum [4].

An optimisation algorithm based on a downhill simplex minimisation technique [5-6] was used to rapidly determine the optimal stack structure for each of the examples described without the need to sample every unique permutation of films and film thicknesses. Typically, optimised structures were calculated using a standard laptop computer, with most calculations being completed within several seconds. In every example the direction of the incident light is through the

backside of the soda-lime glass (SLG) substrate.

3. Results

3.1. Development of film side anti-reflection coating (FSARC) for use with TCO single layers.

Commonly, anti-reflection coatings are applied to the front-side surface of transparent substrates to eliminate the reflectance from the air-substrate interface (e.g. eyeglass lenses). However, for a single film on a transparent substrate a significant reflectance component is also generated at the substrate-film and film-air interfaces. The magnitude of these reflectances can be dramatically reduced by incorporating a multi-layer structure of alternating high/low refractive index layers between the substrate and the film, i.e. a film side anti-reflection coating (FSARC). The effect of incorporating an N layer ZnS/SiO₂ FSARC between a soda-lime glass substrate and a 1000 nm thick TCO film of Al doped ZnO (AZO) was modelled.

Figure 1 shows the average reflectance, over the wavelength range 0.3 – 0.9 μm , from a SLG/FSARC/AZO structure as layers of ZnS and SiO₂ are added in an alternating manner (starting with ZnS) to the FSARC. For each layer a minimum and maximum limit to layer thickness was specified within the model as 5 nm and 100 nm respectively. For each point in the plot the optimisation algorithm was used to minimise reflectance. A two layer ZnS/SiO₂ FSARC was shown to reduce the reflectance of a single film of AZO on SLG from 0.13 to 0.7 (i.e. almost half). A minimum reflectance of 0.6 was achieved

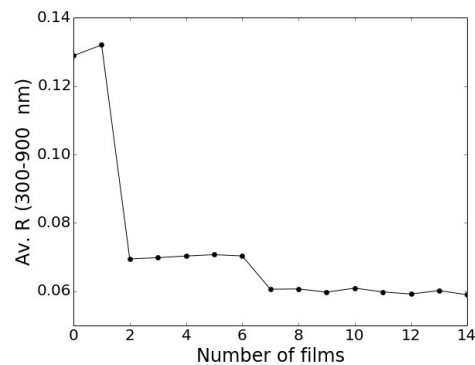


Figure 1: Reduction in average reflectance from AZO layer on soda lime glass due to ZnS/SiO₂ stack of N films.

N	Material	d (nm)
0	SLG substrate	semi-infinite
1	ZnS	5.0
2	SiO ₂	79.2
3	ZnS	23.6
4	SiO ₂	16.1
5	ZnS	12.3
6	SiO ₂	13.8
7	ZnS	26.0
8	SiO ₂	18.9
9	ZnS	10.1
10	AZO	1000

Table 1: Optimised ZnS/SiO₂ FSARC configuration for reduction of reflectance from 1000 nm thick ZnO:Al layer (5 Ω/sq).

for a 9 layer FSARC, the configuration of which is shown in table 1. Figure 2 shows the difference in the transmission spectra obtained for a 1000 nm AZO layer (sheet resistance of 5 Ω/sq) without a FSARC and with the optimised 9-layer FARC detailed in table 1. A clear improvement in the optical response is demonstrated.

The majority of the remaining reflectance was due to the backside air-substrate interface and so the addition of further SiO₂/ZnS layers did not yield a reduction in reflectance.

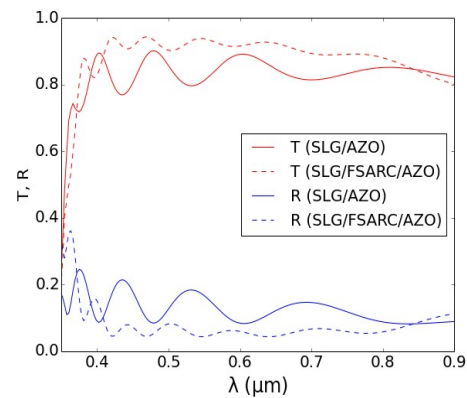


Figure 2: Comparison between transmittance and reflectance spectra for SLG/AZO and optimised SLG/FSARC/AZO configurations.

3.2 Incorporation of FSARC into conventional CdTe solar cell device structure.

The example above can be extended within the context of a full thin-film CdTe solar cell structure. With a starting

configuration of SLG/AZO/CdZnS/CdTe, an N layer FSARC was incorporated between the SLG and AZO to reduce reflectance, the objective being to maximise the light transmitted to the CdTe absorber layer ($E_g = 1.41$ eV) and in-turn maximise the J_{SC} that can be generated. A $Cd_{(1-x)}Zn_xS$ layer with optimal composition $x=0.55$ was used instead of a conventional pure CdS layer. Previous work has shown that this significantly improves the contribution to the J_{SC} from the blue part of the visible spectrum [7]. Lower limits to the thickness of the AZO and CdS layers were set at 500 nm and 30 nm respectively, it being considered that these would be the lowest values that would yield real working devices should the structures be fabricated. The CdTe absorber layer was modelled as semi-infinite, i.e. 100% of the light transmitted through the CdZnS/CdTe interface was absorbed.

The optimisation algorithm was used to directly maximise the J_{SC} for the structure with an incorporated N layer FSARC. N in the range 0-20 was modelled. The optimal FSARC structure is shown in table 2. Beyond 3 layers (ZnS/SiO₂/ZnS) the J_{SC} could not be reduced further. A relative increase in J_{SC} of 5.9% was achieved by incorporating the optimised FSARC between the SLG substrate and AZO film. The calculated J_{SC} increased from 25.6 mAc^m-² without a FSARC to 27.1 mAc^m-² with an optimised 3 layer FSARC.

Figure 3 shows that the key difference in the transmittance and reflectance spectra between structures with and without the the optimised FSARC is a reduction in the magnitude of the interference fringes in the visible part of the spectrum.

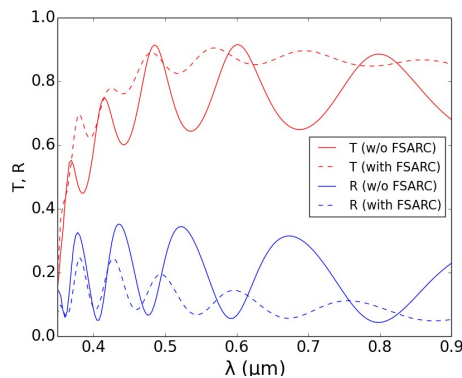


Figure 3: Comparison of transmittance (into semi-infinite CdTe absorber layer) and reflectance for optimised SLG/AZO/CdZnS/CdTe and SLG/FSARC/AZO/CdZnS/CdTe configurations.

N	Material	d (nm)
0	SLG	semi-infinite
1	ZnS	57.6
2	SiO ₂	17.6
3	ZnS	16.0
4	AZO	500.0
5	CdZnS	30.0
6	CdTe	semi-infinite

Table 2: Optimised FSARC structure that yields a maximum J_{SC} value of 27.1 mAc^m-² for a CdTe solar cell configuration.

This yielded an overall reduction in the reflection from the stack's interfaces and and hence an increase in the transmittance into the CdTe absorber layer.

3.3. Viability of ultra-thin Ag films for use as front contact layers in CdTe solar cells.

For common TCO materials conventionally used as contact layers for thin-film PV, e.g. SnO₂:F and ZnO:Al, the achievable limits of free carrier concentrations and mobility generally mean that sheet resistances < 10-15 Ω/square are difficult to achieve without using excessively thick layers (> 1000 nm). This in turn limits the minimum achievable device series resistance (giving rise to reduced diode fill factors, *FF*) and reduces the maximum achievable J_{SC} because of the higher reflectance associated with the large number of interference fringes caused by thick layers, and increased absorption.

The use of ultra-thin (< 10 nm), transparent metal films as contact layers in thin film solar cells presents an opportunity to dramatically reduce the sheet resistance while maintaining high transmittance at visible wavelengths. Here we use the TMM implementation to determine the viability of incorporating a reported Cu/Ag bi-layer [8] for use as a front contact in the CdTe cell configuration

Table 3 shows the configuration of the structure modelled. A 2 nm thick SiO₂ layer was included as the first layer. This would be necessarily experimentally to provide a clean, smooth surface for metal deposition on an SLG substrate. A 1 nm thick Cu 'seed' layer was also included prior to the Ag layer as this has been demonstrated [8] to ensure smooth Ag films with small grain sizes.

N	Material	d (nm)
0	SLG substrate	semi-infinite
1	SiO ₂	2
2	Cu	1
3	Ag	6
4	AZO	5
5	CdZnS	30
6	CdTe	semi-infinite

Table 3: CdTe cell structure incorporating an ultra-thin Ag layer as a transparent conducting contact layer. The configuration yields a calculated J_{sc} value of 27.2 mAcm⁻².

Such films permit the attainment of low resistivities ($< 10^{-7}$ Ω.cm) compared to Ag films without a Cu layer. An intermediate 5 nm thick AZO layer is included between the Ag and CdZnS layers to help limit diffusion of Ag to the CdZnS/CdTe interface which would likely have a negative impact on the electrical performance of a real device.

Figure 4 shows the transmittance into the CdTe absorber layer and the reflectance from the stack. A J_{sc} value of 27.2 mAcm⁻² was calculated for the configuration which is comparable to the optimised FSARC incorporated device structure, based on a conventional 10 Ω/square AZO layer, detailed in section 3.2. However, according to ref. 8, the achievable sheet resistance of the Cu/Ag bi-layer would be < 1 Ω/square, i.e. at least an order of magnitude lower than that provided by a conventional TCO contact layer. This could potentially yield devices with significantly reduced series resistances, higher FF values and in turn, higher achievable conversion efficiencies.

4. Conclusions

An open source implementation of the transfer matrix method has been demonstrated in the context of optical optimisation of CdTe solar cells. It has been demonstrated that the average reflectance (0.3-0.9 μm) from an SLG/AZO interface can be more than halved by incorporating a 9 layer front side anti-reflection coating between the substrate and the AZO. Furthermore, such FSARC structures can be used in the context of conventional CdTe cell structures, e.g. SLG/FSARC/AZO/CdZnS/CdTe, to achieve a 6% relative gain in J_{sc} .

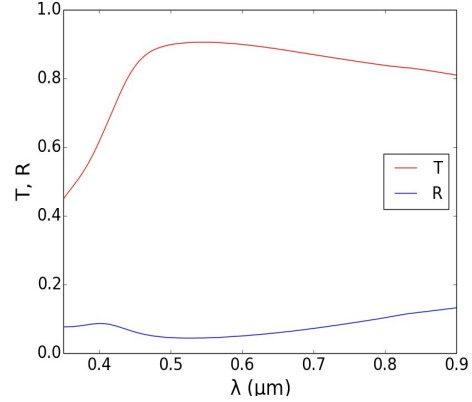


Figure 4: T at CdS/CdTe interface of a glass/SiO₂/Cu/Ag/ZnO/CdS/CdTe stack (configuration shown in table 3). R for the structure is also shown.

The subsequent gain in cell efficiency that this affords is marginal compared to the potential gains achievable through engineering the electronic properties of the constituent films (most particularly the CdTe absorber). Nonetheless, the FSARC strategy will be of importance for high efficiency devices ($>15\%$) where any incremental gains in conversion efficiency are highly prized.

The TMM implementation determined that the use ultra-thin Ag films for use as transparent contact layers in CdTe solar cells is capable of matching the achievable J_{sc} values of conventional TCO based structures. However, the likely attainment of significantly reduced sheet resistances for will provide a route to improvement of cell fill factors and in turn cell efficiency. The optimized cell structures in this work should now be verified experimentally to validate the TMM implementation.

References

- [1] H. A. Macleod, "Thin-Film Optical Filters", Third Ed., (2001), CRC press.
- [2] M. N. Polyanskiy, "Refractive index database", <http://refractiveindex.info> (accessed Mar. 30 2016)
- [3] R. E. Treharne, "RF magnetron sputtering of transparent conducting oxides and CdTe/CdS solar cells", PhD Thesis, University of Durham, (2011).
- [4] "Reference solar spectrum irradiance: Air mass 1.5", NREL, <http://redc.nrel.gov/solar/spectra/am1.5/>, (accessed Mar. 2016).
- [5] J. Nelder, R. Mead, The Computer Journal, (1965), 7(4), 308-313
- [6] SciPy documentation, scipy.optimize.minimize, <http://docs.scipy.org/doc/scipy/reference/generated/scipy.optimize.minimize.html>, accessed Mar. 30 2016.
- [7] R. E Treharne, L. Phillips, A. Clayton et al. Proc. Of IEEE PVSC 40, (2014), 1722-1725
- [8] N. Formica, D. Ghosh, A. Carrilero et al. ACS App. Mat. & Interf., (2013), 5(8), 2048-53